FULL PAPER

Redox Reactions at Cu,Ag/Ta_2O_5 Interfaces and the Effects of Ta_2O_5 Film Density on the Forming Process in Atomic Switch Structures

Tohru Tsuruoka, Ilia Valov, Stefan Tappertzhofen, Jan van den Hurk, Tsuyoshi Hasegawa, Rainer Waser, and Masakazu Aono*

Cu and Ag redox reactions at the interfaces with Ta_2O_5 and the impact of Ta_2O_5 film density on the forming process of Cu,Ag/Ta_2O_5/Pt atomic switch structures are investigated. Cyclic voltammetry measurements revealed that under positive bias to the Cu (Ag) electrode, Cu is preferentially oxidized to Cu^{2+}, while Ag is oxidized to Ag^+ ions. Subsequent negative bias causes a reduction of oxidized Cu (Ag) ions at the interfaces. The diffusion coefficient of the Cu and Ag ions in the Ta_2O_5 film is estimated from the results from different bias voltage sweep rates. It is also found that the redox current is enhanced and the forming voltage of the Cu/Ta_2O_5/Pt cell is reduced when the density of the Ta_2O_5 film is decreased. This result indicates the importance of the structural properties of the matrix oxide film in understanding and controlling resistive switching behavior.

1. Introduction

Owing to significant efforts in the engineering of flash memories, this memory technology is approaching its physical downscaling limit. The prospects for continued downscaling of these memory devices are uncertain, because of reliability issues and cross-talk limitations.[1] Accordingly, alternative emerging memory technologies have attracted much attention in recent years. Redox-based resistive switching memory (ReRAM), based on cation migration in thin film metal oxides, is considered to be a promising candidate for next-generation nonvolatile memories. This is due to metal oxides being highly compatible with current complementary metal-oxide-semiconductor fabrication processes, in addition to its superior characteristics such as fast operation,[2] low power consumption, and potentially excellent scalability.[3] This type of ReRAM is generally referred to as an electrochemical metallization (ECM) cell[4,5] or a conductive bridge memory (CBRAM) cell.[6] Because of its similarity to the "gap-type atomic switch" switching mechanism, in which resistance across a nanometer gap between a mixed conductor electrode and an inert counter electrode is controlled by the formation and dissolution of a metal bridge under bias voltage sweeping,[7] we refer to cation-migration-based ReRAM as "gapless-type atomic switch."[8] Ag/Ta_2O_5-based, gapless-type atomic switches displayed conductance quantization, thus demonstrating the formation of a single point contact in a thin oxide film, which is similar to what occurs in gap-type atomic switches.[9,10]

Oxide films formed by any physical vapor deposition method typically exhibit nanoporous structures, with densities lower than the bulk state,[11] which can absorb moisture from the ambient atmosphere. In previous work, we examined the switching characteristics of Cu/Ta_2O_5/Pt and Cu/SiO_2/Pt cells as a function of ambient water vapor pressure.[12] It was found that absorbed water forms a hydrogen-bond network at the grain boundaries in oxide films and affects the migration of Cu ions as well as the Cu anodic oxidation process. The strength of the hydrogen bonds between hydroxyl groups and the surface of the oxide grains may play a crucial role in determining switching behavior. Recently, Tappertzhofen et al. made comprehensive studies of the redox processes at Cu/SiO_2 interfaces using cyclic voltammetry (CV) techniques.[13,14] The current peaks observed in CV curves were identified with partial redox electrochemical reactions of Cu at the interface. This research group also reported that an open-circuit voltage (i.e., electromotive force, emf), generated by chemical and electrochemical processes and charge distribution during the operation of ReRAM, has a strong impact on the dynamic behavior of nanoscale memories, including anion-migration-based valence charge memory (VCM) cells.[15] The origin of emf in Cu/SiO_2/Pt cells was found to arise from a counter reaction that generates charges by the reduction of moisture at the SiO_2/Pt interface, in parallel with the creation of metallic cations at the Cu/SiO_2 interface.[16]

Dr. T. Tsuruoka, Dr. T. Hasegawa, Dr. M. Aono
International Center for Materials Nanoarchitectonics (WPI-MANA)
National Institute for Materials Science (NIMS)
1-1 Namiki, Tsukuba 305-0044, Japan
E-mail: Tsuruoka.Tohru@nims.go.jp
Dr. T. Tsuruoka, Dr. T. Hasegawa
Core Research for Evolutional Science and Technology (CREST)
Japan Science and Technology Agency (JST)
5 Sanbancho, Chiyoda-ku, Tokyo 102-0075, Japan
Dr. I. Valov, Prof. R. Waser
Peter Gruenberg Institute (Electric Materials)
Forschungszentrum Jülich, 52425 Jülich, Germany
Dr. I. Valov, Dr. S. Tappertzhofen, Dr. J. van den Hulk, Prof. R. Waser
Institut für Werkstoffe der Elektrotecknik 2 (IWE2)
RWTH Aachen, 52074 Aachen, Germany

DOI: 10.1002/adfm.201500853

Compared to SiO_2, the structural properties of deposited Ta_2O_5 and its impact on the resistive switching characteristics of their atomic switches have not been intensively investigated. Chu et al. reported the structural properties of Ta_2O_5 films sputtered at room temperature under different radiofrequency (RF) powers, and their resistance to corrosion by chemicals such as an HF solution.[17] They found that the film becomes dense for higher RF powers, which indicates that the structure of Ta_2O_5 films depends strongly on the deposition conditions. Here, we report a detailed analysis of the redox processes of the interfaces between active metal electrodes (Cu and Ag) and a Ta_2O_5 film by means of CV measurements. In addition, we examined the effects of the structure of Ta_2O_5 films on the redox reactions and on their atomic switch forming operations. The Ta_2O_5 film density varied as a result of the different deposition methods employed and the different deposition conditions. We discuss how the structural properties of the matrix oxide film affect the redox processes in the atomic switch structure.

2. Results and Discussion

Cu,Ag/Ta_2O_5/Pt cells were fabricated on a SiO_2/Si substrate, in which the Ta_2O_5 film was deposited by electron-beam (EB) deposition and RF sputtering. Here, we mainly discuss the results for cells with EB deposited film, because these cells could be measured most stably under a variety of conditions. **Figure 1** shows the typical CV curves of (a) Cu/Ta_2O_5/Pt and (b) Ag/Ta_2O_5/Pt cells obtained for the first (blue curve) and second (red curve) sweep cycles. The current depended on the junction area, therefore, the current density is plotted in this paper. The maximum sweep voltage for positive bias V_+ was limited to avoid a forming process (the first SET operation from a high-resistance (OFF) state to a low-resistance (ON) state), which corresponds to the formation of a metal filament between the top and bottom electrodes by the inhomogeneous nucleation (or electrodeposition) of metal on Pt.[18,19] If the bias voltage was swept beyond 2 V for the Cu/Ta_2O_5/Pt cell and 0.3 V for Ag/Ta_2O_5/Pt cell, the forming process occurred, and resistive switching behavior was subsequently observed under repeated sweeping of the bias voltage. Very low sweep rates were required for the Ag/Ta_2O_5/Pt cell to observe the current peaks clearly. Because an appropriate reference electrode is not used in the measurements, it is difficult to precisely assign the observed current peaks to specific redox reactions. Indeed, the current peak positions changed from cell to cell, although the shapes of the CV curves were almost identical. The current peaks in the positive (negative) sweep direction are associated with the oxidation (reduction) processes at the anode interface.[20] In general, we could clearly observe two oxidation current peaks and two reduction current peaks in the Cu/Ta_2O_5/Pt cell, and one oxidation current peak and two reduction current peaks in the Ag/Ta_2O_5/Pt cell, as indicated by $j_{p,ox1}$, $j_{p,ox2}$, $j_{p,red1}$, and $j_{p,red2}$ in Figure 1.

In aqueous solutions, the standard redox potentials for Cu are given as Cu^+/Cu ($E^{\varphi,1}$ = 0.52 V), Cu^{2+}/Cu ($E^{\varphi,2}$ = 0.34 V), and Cu^{2+}/Cu^+ ($E^{\varphi,3}$ = 0.16 V).[21] Since water is absorbed from the atmosphere into the nanoporous structure of Ta_2O_5,[12] the residual water may involve redox reactions at the interface and

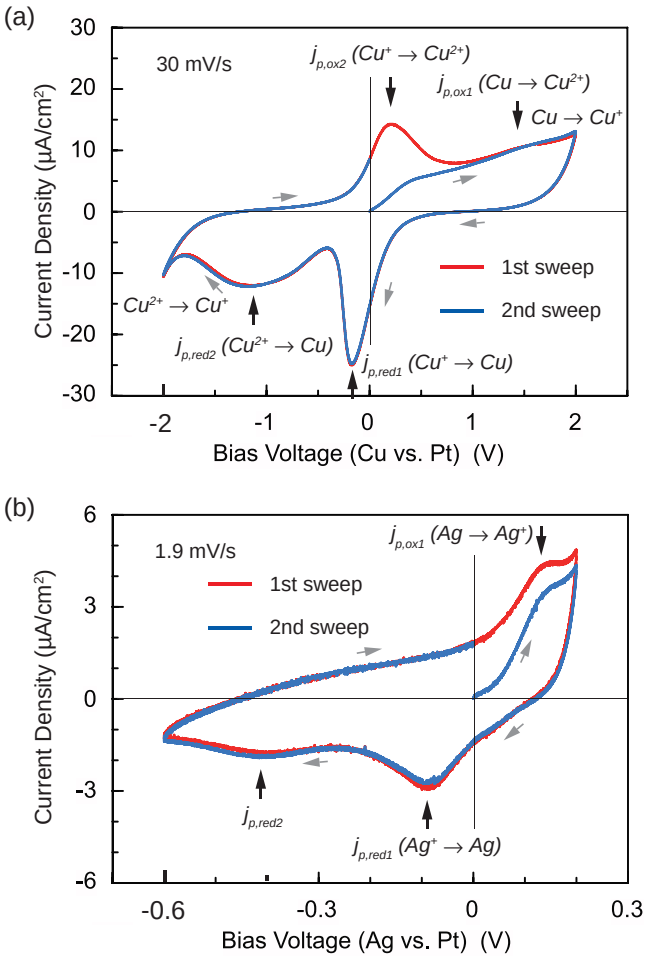

Figure 1. Cyclic voltammogram obtained for the first sweep (blue curves) and the second sweep (red curves) for a) CuTa_2O_5/Pt and b) Ag/Ta_2O_5/Pt cells.

the general trend of redox potentials also holds in our cells. According to the standard redox potentials, oxidation from Cu^+ to Cu^{2+} is thermodynamically the most favorable. However, no Cu ions exist in Ta_2O_5 in the initial state. As the bias voltage is swept from 0 V to the positive sweep direction, Cu should be first oxidized to Cu^{2+}. Therefore, the current peak $j_{p,ox1}$ in Figure 1a is attributed to this reaction. Oxidation from Cu to Cu^+ should take place after $j_{p,ox1}$. The current peak for this reaction may be beyond the maximum sweep voltage in positive bias V_+ (2 V), but this was difficult to observe due to a rapid increase of the electronic contribution. When the bias voltage is subsequently swept back to the negative sweep direction, the reduction from Cu^+ to Cu first occurs because of its lowest reduction energy, and the current peak $j_{p,red1}$ can be assigned to this reaction. As the bias voltage was swept further to the negative sweep direction, a second current peak $j_{p,red2}$ appeared, which is identified as the reduction from Cu^{2+} to Cu. The Cu^{2+} ions may also be reduced to Cu^+ ions after $j_{p,red2}$. In the subsequent sweep cycle, the Cu^+ ions can be first oxidized to Cu^{2+} ions, because a portion of the generated Cu^+ ions remain in the Ta_2O_5 layer after the first sweep cycle. Thus, the current peak $j_{p,ox2}$ corresponds to this reaction. The peak $j_{p,ox2}$ always

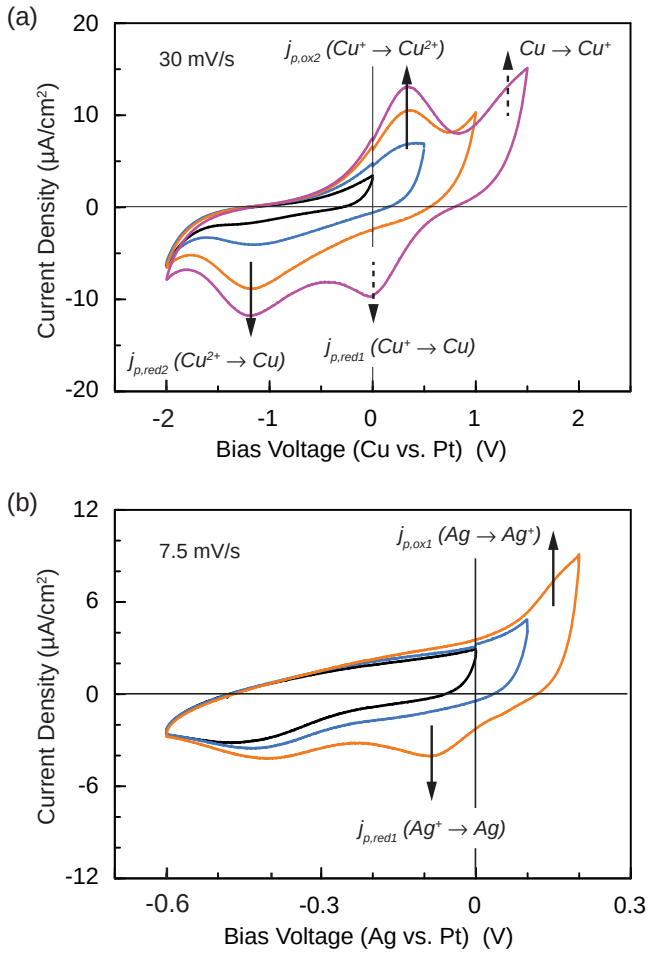

Figure 2. Typical CV curves measured in different voltage sweep ranges for a) $Cu/Ta_2O_5/Pt$ and b) $Ag/Ta_2O_5/Pt$ cells. All the curves were obtained from the second sweep cycle.

appeared after the second sweep cycle, as seen in Figure 1a, which supports the assignment of this current peak. Similar CV curves were also observed for $Cu/SiO_2/Pt$ cells.[13,14]

To determine the validity of the above peak assignments, the CV curves were measured by changing the voltage sweep range, as shown in **Figure 2**a. V_+ was increased from 0 to 1.5 V in increments of 0.5 V, while V_- was fixed at –2 V. All the CV curves in Figure 2 were taken from the second sweep cycle. When the voltage sweep range was between –2 and 0 V, no current peak was observed, indicating that almost no reaction takes place in the negative bias sweep alone. As V_+ was gradually increased, an oxidation current peak $j_{p,ox2}$ (Cu^+ to Cu^{2+}) appeared and, in response to this, a reduction current peak $j_{p,red2}$ (Cu^{2+} to Cu) appeared, as indicated by the solid arrows. This suggests that Cu is preferentially oxidized to Cu^{2+} for smaller bias voltages. As V_+ was increased further, more Cu^+ ions were generated by oxidation from Cu to Cu^+. In response to this, a $j_{p,red1}$ (Cu^+ to Cu) reduction current peak appeared, as indicated by the dashed arrows. The behavior of the CV curves in Figure 2a fully supports the above current peak assignments.

The standard redox potentials for Ag in aqueous solutions are given as Ag^{2+}/Ag^+ ($E^{\varphi,1}$ = 1.98 V) and Ag^+/Ag ($E^{\varphi,2}$ = 0.8 V).[21] Ag-related redox reactions have higher (more positive) equilibrium potentials compared to Cu-related redox reactions. This means that Cu would be more easily oxidized than Ag in positive bias while Ag would be more easily reduced than Cu in negative bias. As the bias voltage was swept from 0 V to the positive sweep direction, Ag was oxidized to Ag^+ owing to its lowest oxidation energy. Therefore, the current peak $j_{p,ox1}$ in Figure 1b can be attributed to this reaction. Because the potential for the oxidation from Ag^+ to Ag^{2+} is much higher than that for oxidation from Ag to Ag^+, the former reaction may be negligible under the voltage sweep range used. When the bias voltage was swept back from V_+ to the negative sweep direction, the current peak $j_{p,red1}$ appeared. Figure 2b depicts CV curves measured with varied voltage sweep ranges. V_+ was increased from 0 to 0.2 V in increments of 0.1 V, while V_- was fixed at –0.6 V. The current peak $j_{p,red1}$ increased with increasing V_+, in response to the increase of the oxidation peak $j_{p,ox1}$ (Ag to Ag^+). Thus, the peak $j_{p,red1}$ is assigned to the reduction from Ag^+ to Ag. As the bias voltage was swept further to negative bias, another current peak $j_{p,red2}$ appeared. It is difficult to attribute this second peak to the reduction from Ag^{2+} to Ag^+, because only Ag^+ ions are generated in the positive voltage sweep and no peak corresponding to the oxidation from Ag^{2+} to Ag^+ was observed, unlike in the $Cu/Ta_2O_5/Pt$ cell. The origin of this second peak is not well understood, and further investigation is needed to identify it.

From a comparison between the results for two active electrodes, it is found that Cu is oxidized preferentially to Cu^{2+}, but Ag is oxidized to Ag^+ under the positive bias voltages used. Cu^+ ions are also produced at higher voltages, both in positive and negative bias, and the CV curves after the second sweep cycles clearly indicated the presence of Cu^+. To construct a comprehensive theoretical model of the resistive switching, both ion species (Cu^{2+} and Cu^+) should be considered in the $Cu/Ta_2O_5/Pt$ cell, but only Ag^+ ions may contribute to the formation of the metal filament in the $Ag/Ta_2O_5/Pt$ cell.

Figure 3 shows the typical variation of CV curves for a) $Cu/Ta_2O_5/Pt$ and b) $Ag/Ta_2O_5/Pt$ cells measured with different sweep rates. Similar to standard redox systems, as the sweep rate increased the current peaks became larger and the peak positions shifted to the higher voltage side in both polarities, as indicated by the dashed arrows. This suggests that an inhibited charge transfer controlled electrode reaction takes place at the $Cu,Ag/Ta_2O_5$ interface.[21] In the case of an inhibited charge transfer at room temperature, the reduction current density can be estimated from the Randles–Sevick equation[21]

$$j_p = 2.99 \times 10^5 \cdot z^{3/2} \cdot c_{ion} \cdot \sqrt{\alpha D v} \quad (1)$$

where D is the diffusion coefficient in $cm^2\ s^{-1}$, c_{ion} the concentration in mol cm^{-3}, z the number of electrons transferred in the redox reactions, α the charge transfer coefficient (for simplicity, we assume α = 0.5),[13] and v the sweep rate in V s^{-1}. Equation (1) suggests a linear relationship between j_p and $v^{1/2}$. **Figure 4**a plots the peak current density of $j_{p,red1}$ as a function of $v^{1/2}$ for $Cu/Ta_2O_5/Pt$ (red open squares) and $Ag/Ta_2O_5/Pt$ (blue open circles) cells. The experimental results are in good agreement with the prediction of Equation (1), as in the case of SiO_2-based cells.[13]

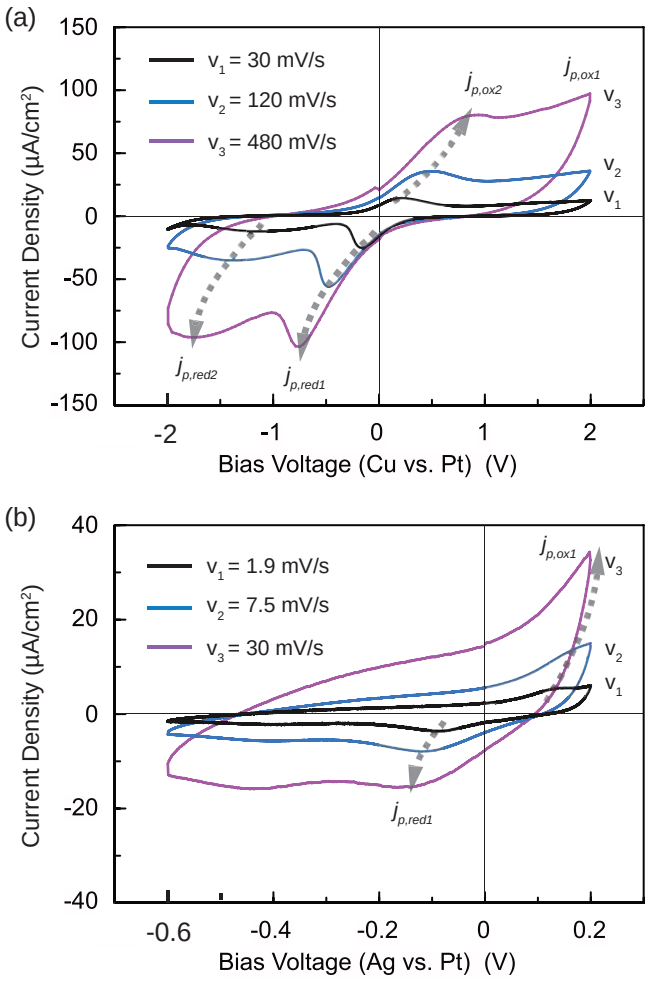

Figure 3. Typical CV curves measured with varied sweep rates for a) Cu/Ta_2O_5/Pt and b) Ag/Ta_2O_5/Pt cells.

To retain the electroneutrality during anodic oxidation, counter charge(s)/reactions are a principal requirement. Water, absorbed into the Ta_2O_5 films from the surrounding ambient atmosphere, can undergo the following reductions at the Ta_2O_5/Pt interface

$$\frac{1}{2}O_2 + H_2O + 2e^- \rightarrow 2OH^- \text{ and/or} \quad (2)$$

$$2H_2O + 2e^- \rightarrow 2OH^- + H_2 \quad (3)$$

as the counter reaction to the oxidation at the Me (Cu or Ag)/Ta_2O_5 interface

$$Me \rightarrow Me^{z+} + ze^- \quad (4)$$

Therefore, the concentration of metal ions (Cu^{z+} or Ag^+) and hydroxide ions (OH^-) must contribute to c_{ion} in Equation (1). Recently, Tappertzhofen et al. found that the latter reduction process (Equation (3)) is more probable for SiO_2-based cells,[22] and we believe that it is also applicable for Ta_2O_5-based cells. Based on this assumption, c_{ion} was estimated from the CV measurements. First, the total generated charge during anodic oxidation was estimated by integration of the current in the positive voltage regime of the first sweep cycle. Then, a mean value of c_{ion} was calculated by taking into account the cell geometry (50 μm × 50 μm × 20 nm). The calculated c_{ion} was plotted as a function of v in Figure 4b. It was assumed that most of the generated ions in the first sweep cycle (Figure 1) are Cu^{2+} ($z = 2$) and Ag^+ ($z = 1$) for each cell. We see that c_{ion} decreases with increasing v for both Cu^{2+} and Ag^+. This can be explained by the time available for the anodic oxidation. At lower sweep rates, more ions can be generated thanks to a longer bias voltage application time. As v increases, the effective oxidation times become shorter, resulting in the decrease of c_{ion}. The concentration of Ag^+ is two or three times lower than that of Cu^{2+} in the observed sweep rate range.

The diffusion coefficient D was calculated using Equation (1) and the results are plotted as a function of v in Figure 4c. At low sweep rates, a higher ion concentration limits further oxidation due to the slower diffusion of cations into Ta_2O_5. As v increases, the anodic oxidation is limited and oxidized ions can diffuse more rapidly in Ta_2O_5. As a result, D is increased with the increase of v. This indicates that the Ta_2O_5 film acts as a concentrating solution and an ion–ion interaction cannot be neglected at higher ion concentrations. D falls in inverse proportion to c_{ion}, as shown in Figure 4d. The diffusion coefficient D can be estimated to be $\approx 10^{-13}$ cm^2 s^{-1} for both Cu^{2+} and Ag^+. There are no available data on the diffusion coefficient of Cu and Ag ions in Ta_2O_5. However, the estimated value of D is about eight orders of magnitude higher than the extrapolated diffusion coefficient of Cu ions, which was evaluated by secondary ion mass spectroscopy for a 120 nm thick Ta_2O_5 film deposited by pulsed laser deposition on Cu.[23] The enhanced diffusion coefficient may come from the downscaling of the film thickness as well as the structural difference of the deposited Ta_2O_5 film. Figure 4d also suggests that Ag ions can diffuse faster than Cu ions at the same sweep rate.

The incorporation of charges separated at both interfaces, $Cu^{z+}(Ag^+)$ at the Cu(Ag)/Ta_2O_5 interface and OH^- at the Ta_2O_5/Pt interface, leading to the formation of an emf within the cell.[15] The theoretical emf voltage V_{emf} cannot be directly measured due to the partial electronic conductivity of the cell. The measurable cell voltage V_{cell} is given by

$$V_{cell} = \frac{R_i^{-1}}{R_i^{-1} + R_{el}^{-1}} V_{emf} \quad (5)$$

where R_{el} is the electronic resistance determined by a leakage current and R_i is the ionic resistance (the equivalent circuit model is depicted elsewhere).[15,16] V_{emf} consists of half-cell reactions at the two interfaces (Nernst potential V_N) and a diffusion potential V_d[15]

$$V_{emf} = V_N + V_d \approx V_0 + \overline{t}_{ion} \frac{k_B T}{2ze} ln(c_{ion}) \quad (6)$$

where V_0 is the standard potential, k_B the Boltzmann constant, e the electron charge, T the absolute temperature, and $\overline{t}_{ion}$ the mean transference number of ions ($\overline{t}_{ion} = \overline{t}_{Me^{z+}} + \overline{t}_{OH^-}$). **Figure 5**a,d shows the time evolution of V_{cell} after the anodic

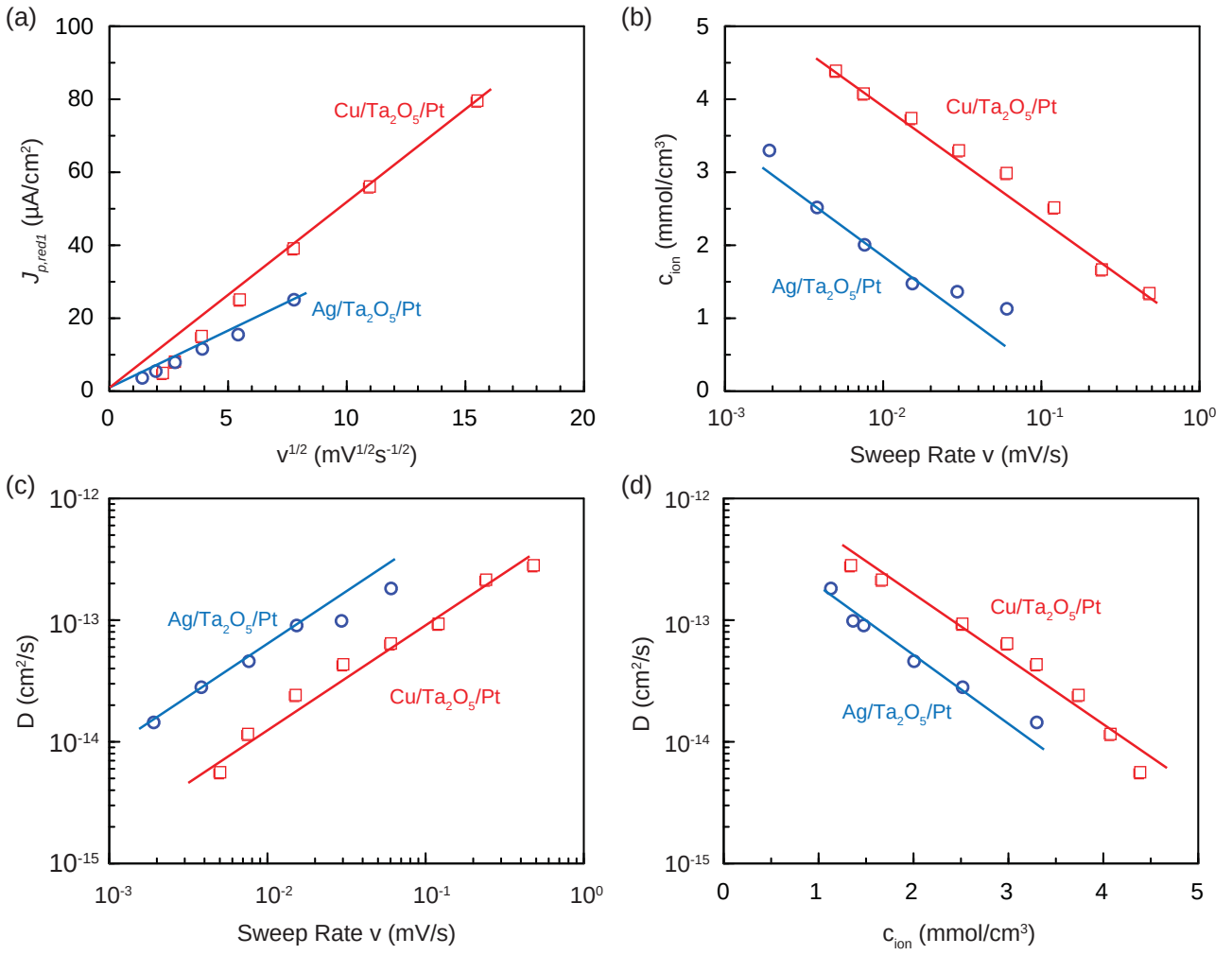

Figure 4. a) Negative peak current $J_{p,red1}$ versus $v^{1/2}$, b) ion concentration c_{ion} versus v, c) diffusion coefficient D versus v, and d) D versus c_{ion}, which were calculated from the CV data and Equation (1).

oxidation for the $Cu/Ta_2O_5/Pt$ and $Ag/Ta_2O_5/Pt$ cells, respectively. The emf measurement was performed, under open-circuit conditions, immediately after the anodic oxidation was taken by sweeping the bias voltage in the positive voltage regime. V_{cell} initially increased for the first ≈70 s and then decreased gradually over time. The increased sweep rates resulted in higher ion concentrations (Figure 4b), and the maximum value of V_{cell} became higher for higher c_{ion}, as shown in Figure 5b,e. A linear relationship between V_{cell} and $\log(c_{ion})$ was obtained, and the transference number $\overline{t}_{ion}$ was estimated to be 0.4 for Ag^+ from the pre-exponential term of Equation (6), which is in good agreement with that estimated for $Ag/SiO_2/Pt$ cells.[15] For the $Cu/Ta_2O_5/Pt$ cell, $\overline{t}_{ion}$ was calculated to be 1.6, which may suggest that the assumption of Cu^{2+} alone is not appropriate. The maximum V_{cell} of the Cu/Ta_2O_5/cell is about one order of magnitude higher than that of the $Ag/Ta_2O_5/Pt$ cell. This is because of smaller concentrations of generated ions than in the $Cu/Ta_2O_5/Pt$ cell, as seen in Figure 4b. Figure 5c,f schematically illustrates how V_{emf} is determined by metal ions and hydroxide ions separated at the respective interfaces under the bias application. The smaller concentration of charges separated at the interfaces results in a faster decrease in V_{cell} for the $Ag/Ta_2O_5/Pt$ cell, as seen in Figure 5d.

It was found that the appearance of redox current peaks depends strongly on the Ta_2O_5 film deposition method. Thus, we investigated the effect of the Ta_2O_5 deposition method (i.e., the structural property) on the redox reactions of Cu ions. Three Ta_2O_5 films were prepared by EB deposition and RF sputtering with different RF power conditions. The average ratio of the number of Ta atoms and O atoms for all the deposited films was estimated to be 0.41–0.42, while the density of the films was found to vary from 6.2 (RF sputtered at 30 W), 7.1 (EB deposited), to 7.6 g cm^{-3} (RF sputtered at 200 W). The fact that the films had almost the same Ta/O ratios but different densities suggests that the obtained Ta_2O_5 films had nanoporous structures with different densities. **Figure 6**a shows typical CV curves measured for $Cu/Ta_2O_5/Pt$ cells with different Ta_2O_5 film densities. For the highest density of 7.6 g cm^{-3}, only electronic current was observed, with almost no ionic current contribution. As the film density decreased, current peaks associated with redox reactions appeared. These ionic current peaks became larger and shifted to the lower voltage side in

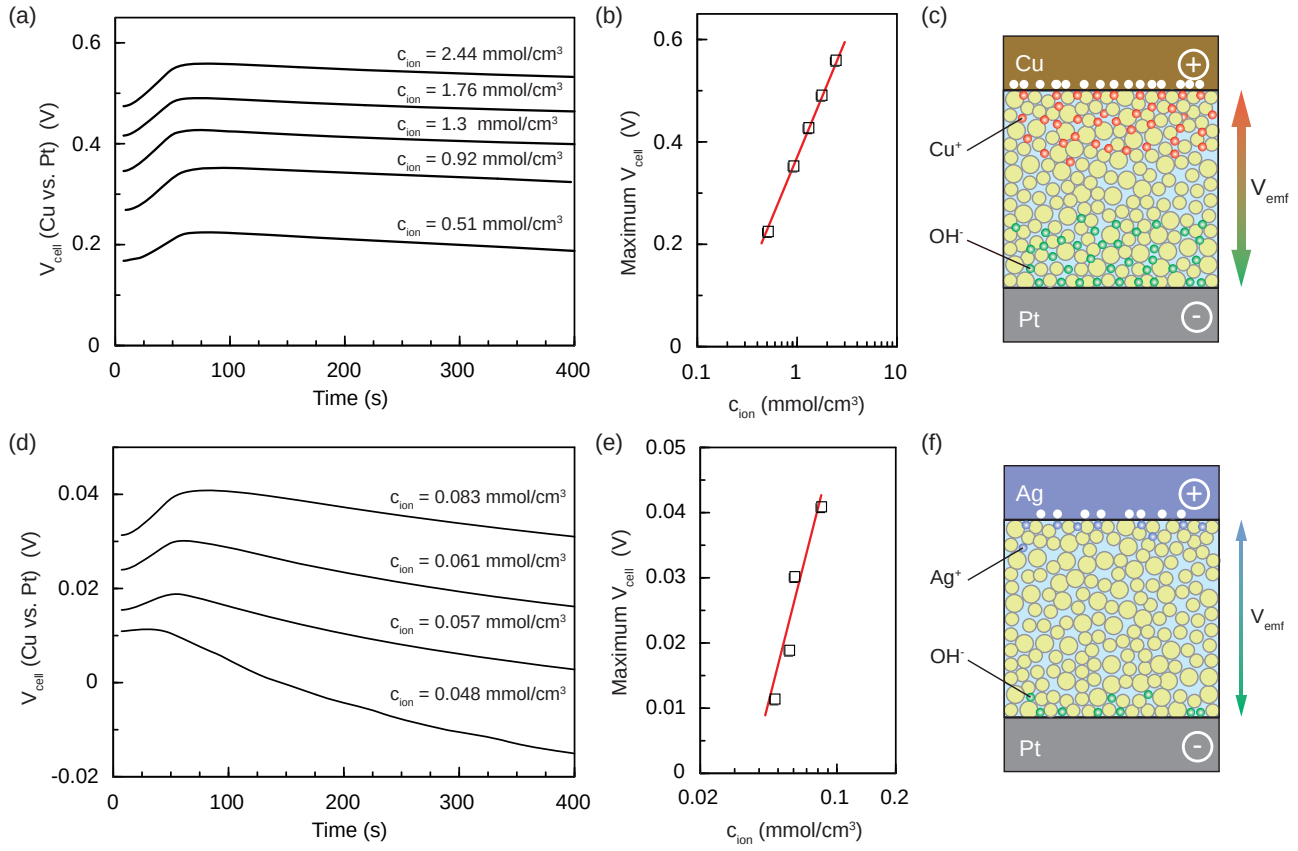

Figure 5. Time evolution of cell voltage V_{cell} measured for different ion concentrations c_{ion} in a) $Cu/Ta_2O_5/Pt$ and d) $Ag/Ta_2O_5/Pt$ cells. The different c_{ion} was adjusted by a single sweep in the positive voltage regime with different sweep rates, as shown in Figure 4b. (b,e) depict the maximum value of V_{cell} plotted as a function of c_{ion}, together with the fitted curves (red lines) calculated using Equation (5). (c,f) schematically illustrate how V_{emf} is determined by ion concentrations generated in the Ta_2O_5 film.

magnitude for the lowest film density of 6.2 g cm^{-3}. This result indicates that the redox reactions are significantly enhanced by lowering the film density.

Film density has a considerable influence on both the redox reaction and the forming process. The corresponding cell forming behaviors are shown in Figure 6b. As the bias voltage was swept beyond V_+, the cells exhibited a forming operation from the OFF state to the ON state at a certain voltage, which is termed the "forming voltage." The forming voltage was found to decrease from 4.3 to 0.44 V with decreased Ta_2O_5 film density, as shown in the inset.

According to the obtained results, we infer the effect of matrix material (Ta_2O_5) film density on the redox reactions in an atomic switch structure, as illustrated in Figure 6c. The deposited Ta_2O_5 films have a nanoporous structure in which small amorphous grains with sizes of less than a few nanometers are randomly piled up. Water molecules, absorbed from the ambient atmosphere into Ta_2O_5, would form a hydrogen-bond network in grain boundaries[12] and in distributed defects such as dangling Ta—O bonds.[24,25] When a positive bias voltage is applied to the Cu or Ag electrode, these active metal atoms are oxidized at the anode interface (Equation (4)) and the generated ions migrate along the grain boundaries, or easier migration paths, toward the Pt electrode. At the same time, in order to maintain the electroneutrality within the cell, water molecules are reduced to OH^- ions at the cathode interface as the counter charge (Equation (3)). The formed emf is dependent on the amount of metal and hydroxide ions generated at the respective interfaces. When the film density is high (such as 7.6 g cm^{-3}), the redox reaction is limited by a small amount of residual water, resulting in a very small ionic current contribution, as seen in Figure 6a. Only a small electronic current was observed at higher bias voltages in both polarities. The Cu ion generation rate is significantly lowered and hence a high bias voltage is required for the forming operation. If the film density is decreased, more water molecules are incorporated into the Ta_2O_5 film, which may enhance the redox reactions at both interfaces, as evidenced by the increased ionic current in Figure 6a. The ionization of Cu at the anode interface is enhanced by chemical oxidation via residual water,[12] and the reduction of water molecules at the cathode interface is also increased by a larger volume of incorporated water. Therefore, more metal ions can be injected into the Ta_2O_5 film, and these ions can migrate faster due to the increased migration paths, as shown in Figure 6c. Thus, the forming voltage is lowered for lower film densities. This result indicates the importance of the structural properties of the matrix film on both the redox reactions and the forming process in the atomic switch structure. The reduction of the electroforming voltage is desirable for practical applications, because a higher forming voltage may

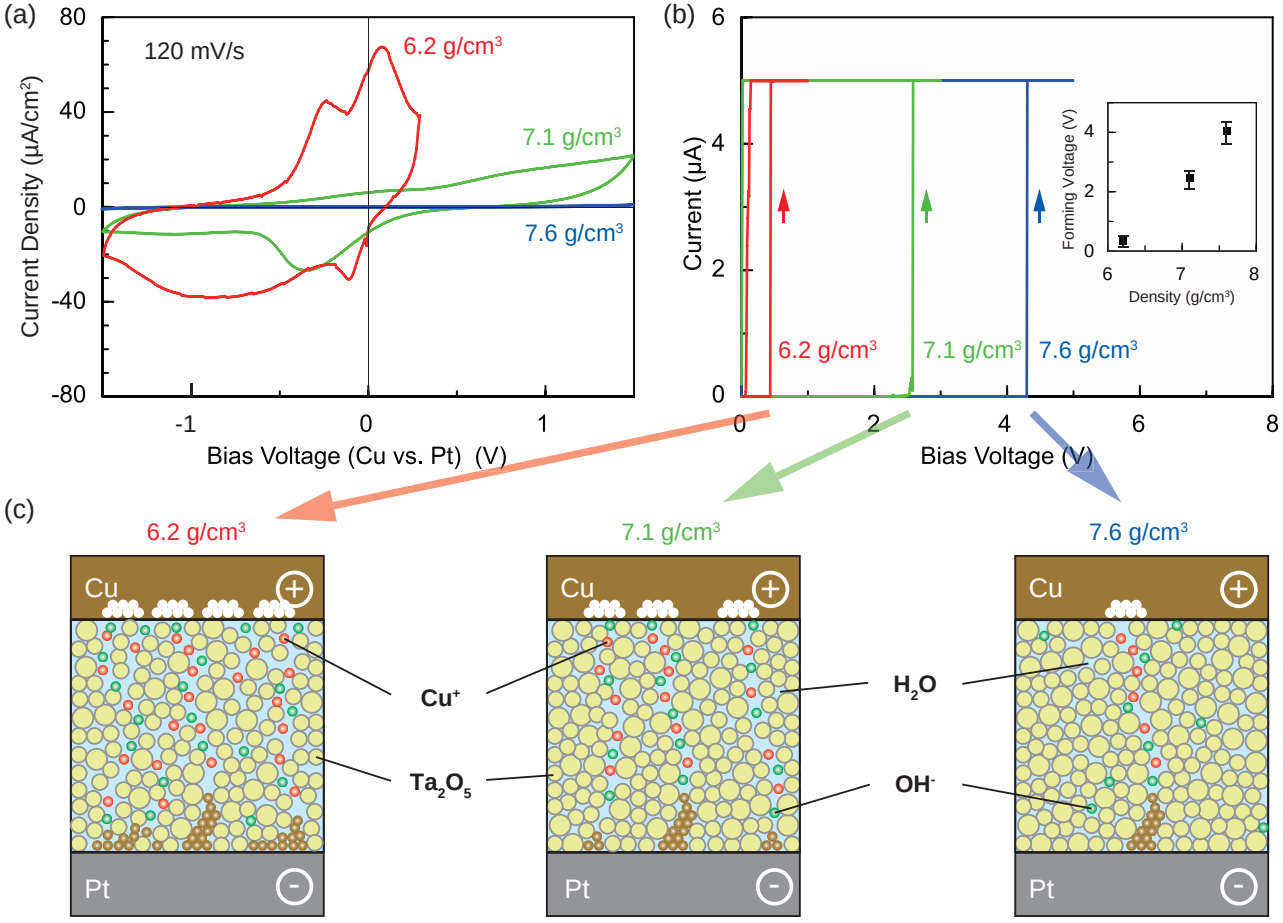

Figure 6. Typical CV curves measured for a) different film densities and b) the forming operation of Cu/Ta_2O_5/Pt cells. The inset plots the forming voltage as a function of the film density. c) Schematic illustration of the impact of Ta_2O_5 film density on the forming process.

cause unwanted damages to oxide-based resistive switching cells.[26] The control of the film density (and the structural property) would overcome this problem. The correlations between the film structure and the resistive switching properties are complicated because they are influenced by many factors such as the deposition conditions of the oxide film and the ambient conditions under measurement. Further detailed investigations are underway to reveal the impact of the film structure on all the characteristics of resistive switching.[25]

3. Conclusions

We have investigated the detailed redox reactions of Cu and Ag at the interface with Ta_2O_5 films by means of CV measurements. It was found that Cu is preferentially oxidized to Cu^{2+} while Ag is oxidized to Ag^+ under positive bias. Subsequent negative bias causes reduction of oxidized Cu (Ag) ions at the interfaces. The diffusion coefficient of Cu and Ag ions in the Ta_2O_5 layer was estimated to be $\approx 10^{-13}$ cm^2 s^{-1}, which is much higher than that estimated for Cu ions in thicker films. The CV results suggest that Ag ions can migrate faster than Cu ions under the same voltage sweep rate, and that the emf is much smaller for an Ag/Ta_2O_5/Pt cell. It was also found that the redox current is enhanced and the forming voltage of a Cu/Ta_2O_5/Pt cell is reduced when the film density of Ta_2O_5 is decreased. This result indicates that Cu (and also Ag) is more oxidized at the interface in a more porous Ta_2O_5 film, which oxidation is assisted by residual water absorbed by the Ta_2O_5 film. The results contribute to a detailed understanding and control of the resistive switching behavior of oxide-based atomic switches and ECM cells.

4. Experimental Section

The Cu,Ag/Ta_2O_5/Pt cells were fabricated on a Si substrate covered with SiO_2 (300 nm). All the layers were deposited at room temperature using metal masks with different patterns. First, 5 nm thick Ti and 30 nm thick Pt were deposited by EB deposition as the adhesion and the bottom electrode, respectively. Then, a 20 nm thick Ta_2O_5 film was deposited by different deposition methods. One film was deposited by EB deposition, with a deposition rate of 0.01 nm s^{-1}. Two other films were deposited by RF magnetron sputtering, using 30 and 200 W RF power, respectively. The average ratio of the number of Ta atoms to O atoms for all the deposited films was estimated from X-ray photoelectron spectroscopy (XPS) measurements. The film density was evaluated from X-ray reflection (XRR) analysis. Finally, 30 nm thick Cu or Ag and 30 nm thick Pt was deposited as the top electrode and the layer protecting against chemical oxidation in air, respectively. Each cell consisted of a cross-point structure with a 50 μm × 50 μm junction area.

The CV measurements were performed in air (at a relative humidity of 20%–30%) at room temperature using a source meter with high input impedance (Keithley 6430). A bias voltage was applied to the top electrode and swept at a constant sweep rate. The sweep rate was varied between 1.9 and 480 mV s^{-1}. The bottom Pt electrode was electrically grounded in all of the measurements. The cell forming behaviors were also observed using the same experimental setup.

Acknowledgements

This work was supported in part by JSPS KAKENHI Grant No. 24350278 and by BMBF Project No. 03×0140. The authors would like to thank A. Besmehn and P. Grewe for the XPS and XRR measurements of Ta_2O_5 films, respectively.

Received: March 3, 2015
Revised: May 11, 2015
Published online: June 1, 2015

[1] N. Chandrasekaran, *IEDM Tech. Dig.* **2013**, 344.
[2] T. Tsuruoka, T. Hasegawa, I. Valov, R. Waser, M. Aono, *AIP Adv.* **2013**, *3*, 032114.
[3] R. Waser, M. Aono, *Nat. Mater.* **2007**, *6*, 833.
[4] I. Valov, R. Waser, J. R. Jameson, M. N. Kozicki, *Nanotechnology* **2011**, *22*, 254003.
[5] I. Valov, *ChemElectroChem* **2014**, *1*, 26.
[6] M. Kund, G. Beitel, C.-U. Pinnow, T. Röhr, J. Shumann, R. Symanczyk, K.-D. Ufert, G. Müller, *IEDM Tech. Dig.* **2005**, 754.
[7] K. Terabe, T. Hasegawa, T. Nakayama, M. Aono, *Nature* **2005**, *433*, 47.
[8] T. Hasegawa, K. Terabe, T. Sakamoto, M. Aono, *MRS Bull.* **2009**, *34*, 929.
[9] T. Tsuruoka, K. Terabe, T. Hasegawa, M. Aono, *Nanotechnology* **2012**, *22*, 435705.
[10] T. Ohno, T. Hasegawa, T. Tsuruoka, K. Terabe, J. K. Gimzewski, M. Aono, *Nat. Mater.* **2011**, *10*, 591.
[11] J. M. Ngaruiya, S. Venkataraj, R. Drese, O. Kappertz, T. P. L. Pedersen, M. Wuttig, *Phys. Status Solidi A* **2003**, *198*, 99.
[12] T. Tsuruoka, K. Terabe, T. Hasegawa, I. Valov, R. Waser, M. Aono, *Adv. Funct. Mater.* **2012**, *22*, 70.
[13] S. Tappertzhofen, S. Menzel, I. Valov, R. Waser, *Appl. Phys. Lett.* **2011**, *99*, 203103.
[14] S. Tappertzhofen, H. Mündelein, I. Valov, R. Waser, *Nanoscale* **2012**, *4*, 3040.
[15] I. Valov, E. Linn, S. Tappertzhofen, S. Schmelzer, J. van den Hurk, F. Lentz, R. Waser, *Nat. Commun.* **2012**, *11*, 530.
[16] S. Tappertzhofen, I. Valov, T. Tsuruoka, T. Hasegawa, R. Waser, M. Aono, *ACS Nano* **2013**, *7*, 6396.
[17] A. K. Chu, M. J. Chuang, K. Y. Hsieh, H. L. Huang, Y. C. Yu, C. W. Wang, E. K. Lin, *J. Electron. Mater.* **1999**, *28*, 1457.
[18] T. Tsuruoka, K. Terabe, T. Hasegawa, M. Aono, *Nanotechnology* **2010**, *21*, 425205.
[19] T. Tsuruoka, K. Terabe, T. Hasegawa, M. Aono, *Nanotechnology* **2011**, *22*, 254013.
[20] A. J. Bard, L. Faulkner, *Electrochemical Methods: Fundamentals and Applications*, John Wiley & Sons, Hoboken **2001**.
[21] A. J. Bard, R. Parsons, J. Jordan, *Standard Potentials in Aqueous Solution*, Marcel Dekker, New York, **1985**.
[22] S. Tappertzhofen, R. Waser, I. Valov, *ChemElectroChem* **2014**, *1*, 1287.
[23] N. Banno, T. Sakamoto, N. Iguchi, S. Sunamura, K. Terabe, T. Hasegawa, M. Aono, *IEEE Trans. Electron Devices* **2008**, *55*, 3283.
[24] T. Dimitrova, E. Atanassova, *Vacuum* **1998**, *51*, 151.
[25] C. Mannequin, T. Tsuruoka, T. Hasegawa, M. Aono, unpublished.
[26] J. J. Yang, F. Miao, M. D. Pickett, D. A. A. Ohlberg, D. R. Stewart, C. N. Lau, R. S. Williams, *Nanotechnology* **2009**, *20*, 215201.